Physics and Chemistry of the Earth xxx (xxxx) xxx

Contents lists available at ScienceDirect

Physics and Chemistry of the Earth

journal homepage: http://www.elsevier.com/locate/pce

Effects of urbanization on precipitation in Beijing

Jingru Liu [a,b], K. Heinke Schlünzen [b], Thomas Frisius [b], Zhan Tian [c,*]

[a] Bao'an Drainage Co.,Ltd, Shenzhen, 518000, China
[b] School of Integrated Climate System Sciences, University of Hamburg, Germany
[c] School of Environmental Science and Engineering, Southern University of Science and Technology, Shenzhen, 518055, China

ARTICLE INFO

Keywords:
Urbanization
Precipitation
METRAS model
Land use
Extreme rainfall

ABSTRACT

Since the 1980s, the industrialization and urbanization of the Beijing area has entered a period of high-speed growth. This paper asks the question: How have such great changes in urban land-use over the past decades impacted urban precipitation? In this study, we investigate and analyze the effects of urbanization on the summer precipitation in Beijing using numerical modeling approaches. Applying the numerical mesoscale atmospheric model METRAS, we determine the impact of surface cover on 13 heavy precipitation events. We implement five idealized land-use scenarios: Reference scenario, No-urban scenario, High-building scenario, Urban-expand scenario, and No-vegetation scenario. There is nearly no difference in the mean precipitation sum across all 13 simulated rain events and between the urban-scenarios and the rural-scenario. We find effects of urbanization on precipitation only in some single cases. We conclude urbanization does effect the local precipitation of Beijing; it reduces rainfall in the urban area and increases rainfall downwind of the city. In some cases, larger percentage of sealed area could give rise to the heavier precipitation or extreme rain events. And we conclude the urban pattern significantly impacts rainfall area and intensity. Increased urban size or density may speed up rain clouds while increased urban height may disrupt or bifurcate the clouds. Our results offer a new viewpoint and further the study of urban impacts on precipitation (UIP). The results are important for sustainable and harmonious development of the economy, society, and environment in Beijing as well as other cities with rapid urbanization.

1. Introduction

The urban system is complex and not only consists of anthropological systems such as societal and economic systems, but also natural systems. Urban area is characterized by an aggregation of population, technique, information, and opportunity. Nowadays the world is experiencing the largest growth of urban areas in history. The 2018 Revision of World Urbanization Prospects produced by the Population Division of the UN Department of Economic and Social Affairs (UNDESA, 2018) notes that 55% of the world's population lives in urban areas, a proportion that is expected to increase to 68% by 2050. A report released by the Chinese National Bureau of Statistics announced that by the end of 2019 the urbanization rate of China had reached 60.6%, which lifted the world's urbanization level to a new height. Now city inhabitants have already experienced advantages of urbanization as well as the disadvantages — crowded traffic, pollution, treacherous public security, and a variety of meteorological and climatological disasters. Precipitation in megacities is a popular issue because of the potential substantial impacts on urban management of flash floods, waterlogging, landslides, and mudflows (Yang et al., 2017), closely connected to the safety of the city's people and property.

Both observational and modeling results in previous studies have indicated that the impacts of urban area on precipitation actually exist, and that their specific properties (e.g., distribution, diurnal variation, seasonal cycle and intensity) also have been widely investigated around the world. Urbanization induced rainfall enhancement in downwind regions occur in many metropolitan areas, such as Oklahoma City (Hand and Shepherd, 2009), Houston (Shepherd and Burian, 2003), Atlanta (Mote et al., 2007), Hamburg (Schlünzen et al., 2010), and Beijing (Zhu et al., 2019). Some numerical modeling studies have also demonstrated the UIP. Sensitivity experiments (Rozoff et al., 2003) in Regional Atmospheric Modeling System (RAMS) show that the urban heat island (UHI) effect plays a key role in initiating deep, moist convection downwind of the city. Meanwhile, many researchers have reported different findings. For instance, Lei et al. (2008) and Niyogi et al. (2011) find that urbanization leads to increased precipitation in the upwind

* Corresponding author.
E-mail address: tianz@sustech.edu.cn (Z. Tian).

https://doi.org/10.1016/j.pce.2021.103005
Received 5 October 2020; Received in revised form 24 February 2021; Accepted 27 February 2021
Available online 4 March 2021

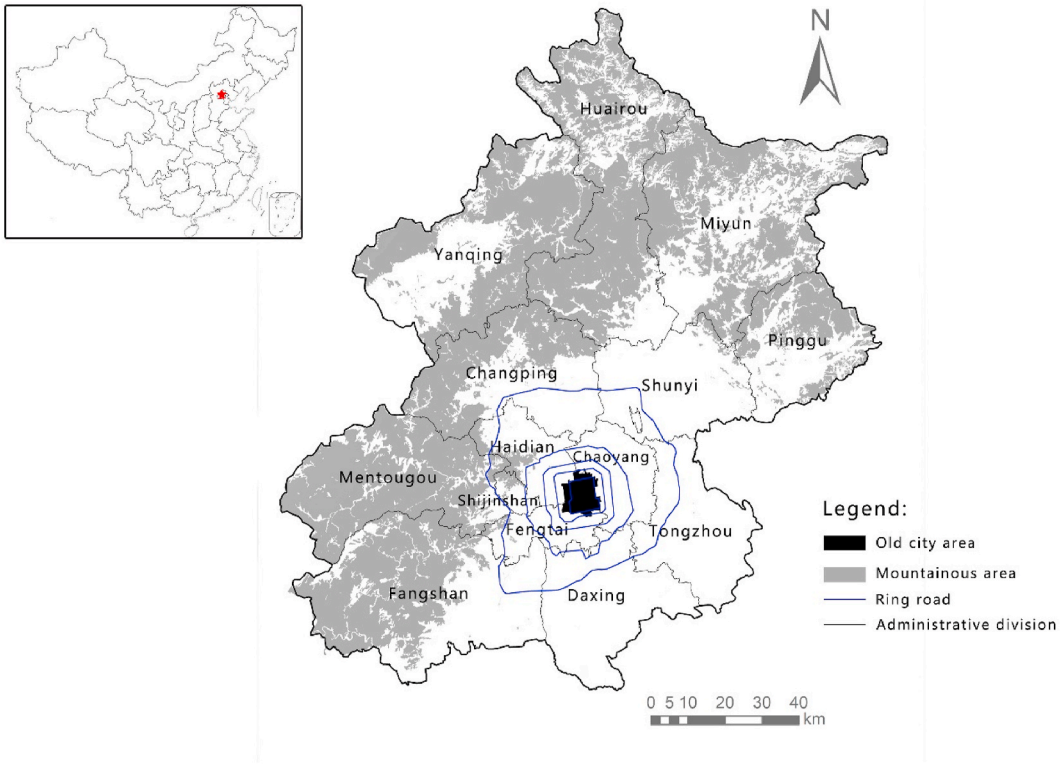

Fig. 1. The study area.

urban region. Another Weather Research and Forecasting (WRF) Model simulation indicates the rainfall area greatly depends on the urban canopy roughness (Xing et al., 2020). Zhang et al. (2020) analyzed the potential physical mechanisms of urban expansion and precipitation and conclude that the leading role of urbanization in the process of precipitation may change with the scale of the city. In addition, Lin (2000) indicated moving thunderstorms show a bifurcated trend and move around the city due to the building barrier effect. Yue et al. (2019) also find the building barrier effect influences local typhoon precipitation in Shanghai. Therefore, the effects of urbanization on precipitation are still argued. Because of the unknowns and uncertainties associated with the precipitation, there is still room for future studies. For example, previous studies have focused on the effects of the increasing urban size on precipitation, limited attention has been paid to the building heights and density (Xing et al., 2020). In addition, since each city differs in structure, climatology, geography and so on, and different models have different simulating approaches, it is quite necessary to explore the urban induced-effects of different cities all around the world with different meteorological models.

For our study, we selected a typical megacity Beijing (sometimes romanized as Peking, 39°28′-41°25′N, 115°25′-117°30′E) for three primary reasons. First, because of Beijing's rapid urbanization over the past decades with built-up area and population increases. Beijing's urban-construction area has increased fourfold from 415.7 km^2 in 1990 (Schneider and Mertes, 2014) to 1603 km^2 in 2017 (China City Statistical Yearbook, 2017). Second, heavy precipitation is one of the major concerns in Beijing, especially after the July 2012 Beijing flood event. Third, the urban precipitation of Beijing has not been investigated well enough. Some previous studies claim that summer rainfall in Beijing has shown an obvious tendency of decline from the 1980s–2000s (Zheng et al., 2008; Zhang et al., 2009), and more precipitation in regions downwind of the city (Sun, 2007; Zhu et al., 2019). Other studies claim the urban area of Beijing has fewer rainy days but higher rainfall intensity compared to its surrounding region (Zhang et al., 2014), and the intense short-duration rainfall events often begin in late evening and nighttime and tend to end in late night and early morning (Yang et al., 2017). Yuan et al. (2020) also found the hourly urban precipitation extremes are increasingly inclined to occurring during night-time, especially during 18:00 LST to 02:00 LST (UCT+8:00). However, most of the previous studies analysis the UIP by using statistical approaches ignoring large-scale climate variability. And the previous numerical modeling studies paid little attention to the effects of urban structures or patterns on precipitation, as well as lack a thorough study of precipitation mechanisms. The aim of this study is to investigate the effects of urbanization on precipitation and especially on heavy precipitation in Beijing by using the mesoscale atmospheric model METRAS. This study will investigate how change in land-use over the past four decades have impacted regional precipitation, explore the influence of different urban patterns on UIP, and compare and analyze climate modifications through a series of sensitivity experiments with different scenarios using idealized numerical modeling. Our urban precipitation investigations are significant for urban and hydrological design, flooding forecasting and control management. Our results are important for sustainable and harmonious development of the economy, society, and environment of Beijing, as well as other cities with rapid urbanization.

2. Study area and methodology

2.1. Study area

Beijing, which is the capital of the People's Republic of China, is located in the Northern China Plain about 150 km from the Bohai Sea. The elevation encompassing Beijing is high in the northwest and low in the southeast. The Taihang Mountain and the Yan Mountain are situated on the western side and northern side of the city respectively. They form a large semicircular mountain cove around the so-called Beijing Plain with a mean elevation of about 40m. Beijing has a typical temperate monsoon climate, characterized by hot, humid summers and cold, dry

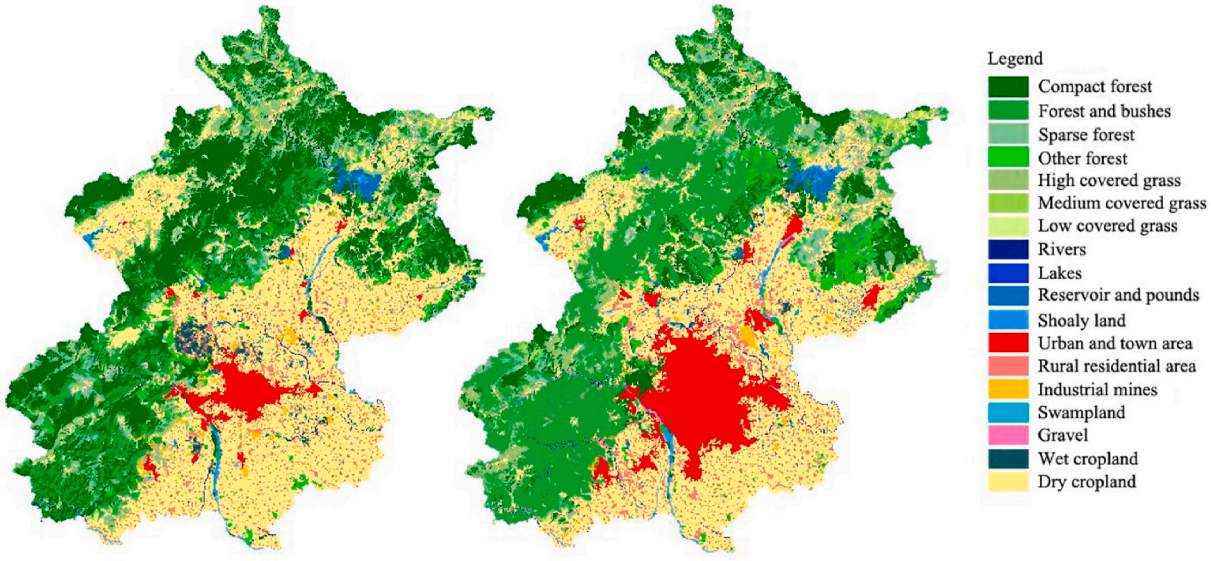

Fig. 2. The land use of Beijing in 1984, 2005 based on the TM images and "Beijing-1" data (Mu et al., 2007).

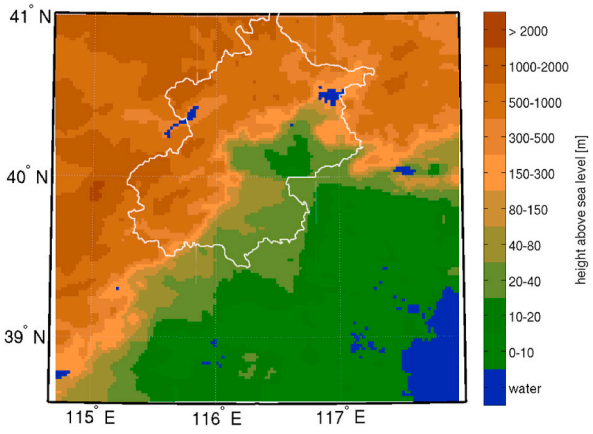

Fig. 3. The location of chosen domain for the simulations, the field shown is one-time filtered topography. The white line circled area stands for Beijing area.

winters. The climatological annual precipitation over the region is about 600–700 mm (Guo et al., 2006), with a great majority of it falling in the summer period.

The Beijing Municipality has a total land area of 16410.54 km^2, with a population density of 1312 people per km^2 by the end of 2019. Currently, Beijing Municipality is composed of urban and suburban districts and two rural counties. Eight of the 14 districts (Xuanwu, Xicheng, Chongwen, Dongcheng, Haidian, Shijingshan, Fengtai, and Chaoyang) are traditionally viewed as the central city area covering about 300 km^2 (He et al., 2006). Surrounding the Forbidden City, from the 2nd Ring Road (1980s) to the 6th Ring Road (2009), a ring pattern road system has developed (Fig. 1), which is ridiculed as making a big "pie". At the same time, the urban area has expanded by about a factor of four since 1980 (Yang et al., 2009). Since the 1980s, the industrialization and urbanization of Beijing has entered a high-speed growth period, which is seen in the change of urban area from 1984 to 2005 (Fig. 2). Three main features of Beijing's urban growth stand out in these two figures. Since urban sprawl is one of the main forms of suburban land development in Beijing after the 1980s (Zhao, 2010), its urban development is both expansionary and sprawling. Suburban regions as well as satellite towns have become highly developed. And numerous small urban patches occur dispersed across all of the Beijing Municipality. Urban Beijing has expanded in all directions except east because of the mountains. Apart from the urban growth features, the figures show other land use changes such as declining area of forests, paddy fields, and marshes.

Table S1, based on the TM images and "Beijing-1" satellite data, gives more detailed information on each type of land use change. Comparing data from 1984, 1996, 2001, and 2005 the most visible change is the continual increase in the urban and town area by occupying farmland and forest areas. Urban and town areas increased from 484.86 km^2 (accounting for 2.96%) to 1496.88 km^2 (9.14%), and the growth rate of urban and town area during the period 1984–1996 was as high as 107.57%. The rural residential area also increased in the long-term, even though there was a decline during 1984–1996.

2.2. METRAS setup for Beijing

2.2.1. Relevant characteristic of METRAS

In this study, we use the mesoscale meteorological model METRAS (Schlünzen, 1990). METRAS is a 3-D model which was formulated in 1980s mainly at the University of Hamburg, and has been widely applied in Germany and abroad. Like other meteorological and climate numerical models, it fulfills conservation of mass, momentum, and energy based on the primitive equations. METRAS uses diagnostic and prognostic equations to get meteorological parameters (e.g., temperature, humidity, pressure, wind speed and direction). It consists of many sub-models, such as the cloud microphysics model which allows for the formation of clouds and precipitation; the chemistry and dispersion model which allows for the calculation of pollutant dispersion; the sea ice model which gives a more accurate energy budget. The anelastic and Boussinesq approximations as well as other approximations are applied in the METRAS model (Grawe et al., 2013). In addition, the model can realize sub-grid-scale surface cover representation. The surface coverage or characteristics determine the surface dependent fluxes which have an effect on the lower atmosphere. METRAS has 56 surface cover classes with corresponding physical parameters. However, there is no canopy sub-model in the model, so the variation characteristic of turbulent kinetic energy flux and effects of building structures on momentum and turbulent length scales are unaccounted for. Therefore, the surface fluxes we calculate cannot completely represent the real effects of underlying surface and anthropogenic activities.

Table 1
List of heavy precipitation events and their meteorological parameters.

Event	Date	Near surface air temperature [°C]	Water & soil temperature [°C]	Dry days [d]	Wind direction around 700 hpa level
1	Jun 15, 2001	20.0	20	0	SW
2	Aug 04, 2002	30.6	25	0	NW
3	Jul 20, 2004	25.8	25	1	SW
4	Jul 10, 2005	30.7	23	0	NW
5	Aug 05, 2005	28.1	26	0	NW
6	Jul 12, 2006	28.0	24	1	SW
7	Aug 01, 2007	30.0	26	0	NW
8	Aug 12, 2007	28.5	26	4	NW
9	Jul 04, 2008	31.0	25	2	SW
10	Aug 11, 2008	25.6	28	0	SW
11	Aug 30, 2010	28.7	25	8	NW
12	Aug 14, 2011	26.4	26	4	SW
13	Aug 26, 2011	21.3	26	9	SE

Table 2
Land use scenarios investigated in the study.

Experiment	Name of Scenarios	Land Use Data Used
Control experiment	Reference scenario (SCE_Refer)	The land use data of 2006 for whole Beijing is used.
Sensitivity experiment	No-urban scenario (SCE_Nourb)	The urban area is replaced by cropland.
	High-building scenario (SCE_High)	The low building class is replaced with the high building class.
	Urban-expand scenario (SCE_Expand)	All grid cells with 10–60% of urban class are replaced by grid cells with 60% of urban class. The other grid cells remain the same.
	No-vegetation scenario (SCE_Noveg)	All the vegetation in the urban area (more than 30% of urban class in one grid) is removed, and replaced by buildings.

2.2.2. METRAS adaptation for Beijing

A model domain with a fixed horizontal grid spacing of 2 km was centered over the Beijing area, and it consisted of 135 × 141 grid points with latitudes from about 38.3° to 41.0°N, longitudes from about 114.4° to 118.0°E. There are 38 vertical levels, which are set with variable grid spacing in the first 0–6.5 km of the atmosphere and maintained at a spacing of 1.0 km for the height above 6.5 km. The grid spacing close to the surface is 20 m, the lowest model level is located in 10 m above ground. The model top extended to about 16.5 km above the surface to allow very deep convection processes.

The elevations in the model domain were retrieved from the GTOPO30 global data, which is available from the U.S Geological Survey (USGS) Center for Earth Resources Observation and Science (EROS). GTOPO30 is a global digital elevation model with a horizontal resolution of approximately 1 km, providing regional and territory scale topographic data. Fig. 3 shows the topography of the investigated domain. A relatively complex feature of the topography is the high mountains in the north and west and sea in the southeast. The mountains reach up to more than 2000 m above the sea level while the flat terrain's elevation ranges between 0 and 80 m.

Since such large height differences and the rugged mountains are big challenges for the model, we applied a three-point filter method to smooth the orography. The three-point filter equation is:

$$\psi = \frac{1}{4}\left(\psi_{i+1} + 2\cdot\psi + \psi_{i-1}\right) \quad (1)$$

where each output $\dot{\Psi}$ is the scaled average of three successive inputs. The extreme values are modified after the three-point filter, while at the same time the general characteristics of the data can be kept. By using this smoothing method, computational effort was reduced and some spurious effects of the mountains were avoided.

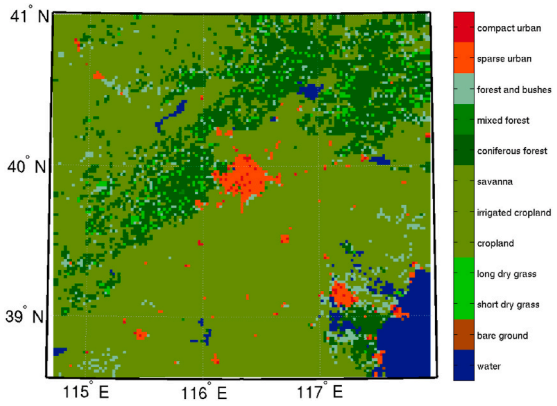

Fig. 4. Main surface cover class of the chosen domain.

The advection and diffusion terms in the Reynold equations are integrated in time by means of the Adams-Bashforth-scheme (Schlünzen et al., 2012). The scheme equation is:

$$\phi^{n+1} = \phi^{n} - \left\{\frac{3}{2}f^{n} - \frac{1}{2}f^{n-1}\right\}\cdot\Delta t \quad (2)$$

where f is the sum of the advection term and the diffusion term. Δt denotes the time step. To ensure the stability of the numerical scheme, the time step should meet the following restriction (Schlünzen et al., 2012):

$$\Delta t \leq 0.9\cdot\left\{\frac{|\overline{u}|}{\Delta x} + \frac{|\overline{v}|}{\Delta y} + \frac{1}{\Delta\eta}\{|w| + |D||\overline{u}| + |E||\overline{v}|\} + \frac{2K_{hor}}{\Delta x^2} + \frac{2K_{hor}}{\Delta y^2} + \frac{2K_{vert}}{\Delta z^2} + v_R\right\}^{-1} \quad (3)$$

where u, v, and w demote the wind speed in the x, y, and z direction respectively. The grid increment in each direction is Δx, Δy and Δz. D and E denote the transformation coefficient for terrain slope in the x and y direction, where D = E = 0 if the terrain is flat. K_{hor} is the horizontal exchange coefficient for momentum and K_{vert} is the vertical exchange coefficient for moment. V_R is the damping coefficient.

Due to the slope of the terrain, one component of the horizontal exchange coefficient for momentum points is in vertical direction. This component is not considered in the time step restriction (Equation (3)). In the area of Beijing, with its complex topography, the slope leads to numerical instabilities. If the terrain slope were considered in Equation (3), the resulting time steps would be very low (e.g., <0.1 s), which would strongly improve the computational performance. Therefore, the horizontal exchange coefficient for momentum K_{hor} is simplified and assumed to be zero in this study. In order to smooth the simulated wind fields, a Shapiro three-point-filter (Equation (1)) is applied to the three components of the wind vector.

2.2.3. Selected heavy precipitation events

In this study, a heavy precipitation event conforms to the following requirements based on the radiosonde sounding data (12:00 UTC, 20:00 CST) from University of Wyoming website: a) Summer rainfall in June–July–August (JJA) happened between the year 2000 and 2011; b) Convective available potential energy is larger than 2000 J. Finally, 13 heavy rainfall events have been selected listed in Table 1.

Besides, according to the daily National Centers for Environmental Prediction (NCEP) sea surface temperature (SST) analysis data and the daily observational data from the German Meteorological Service (DWD), the water temperature, soil temperature and "dry days" of each event have also been used to initialize the one-dimensional version of the METRAS model. We assumed soil temperature to be the same as water temperature. "Dry days" are the total number of the days without

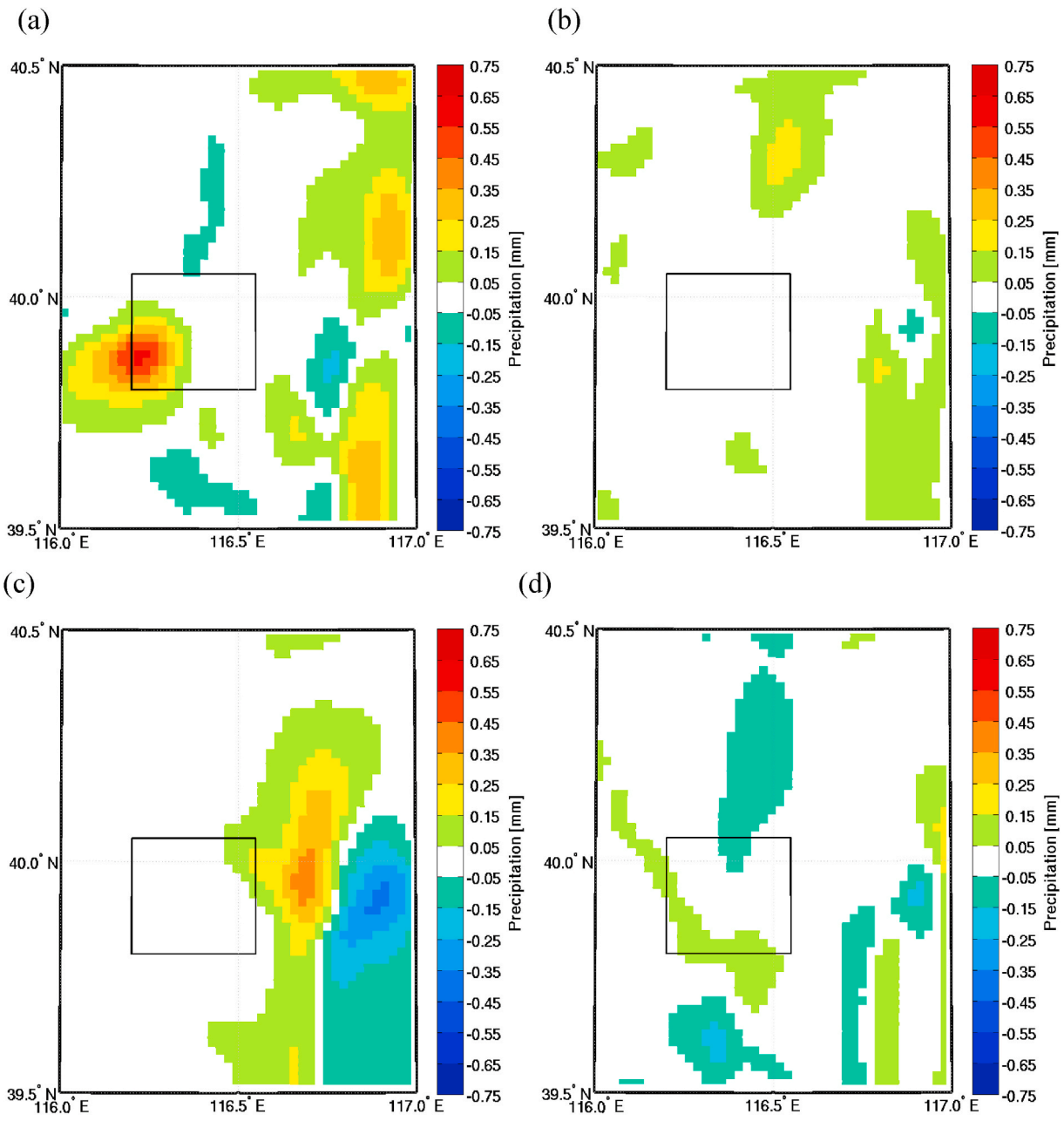

Fig. 5. Difference of the precipitation sum over Day1 and Day2 of all 13 rain events between two scenarios. a) SCE_Refer - SCE_Nourb; b) SCE_High - SCE_Nourb; c) SCE_Expand - SCE_Nourb; d) SCE_Noveg - SCE_Nourb. The framed area is the central city. (Unit: mm).

effective precipitation (>1 mm) before each event. The number of "dry days" impacts the soil moisture, which can alter the latent and sensible heat flux exchanges between the surface and lower atmosphere. Moist soil leads to higher evaporation, causing more precipitation, which in turn feeds back into soil moisture. Taylor et al. (2012) claim that rain falling in the summer afternoon is more likely to occur over drier soil places. Specifying the "dry days" is beneficial to the accuracy of simulations.

Since the sounding data were recorded at 20:00 CST, at which time the convection was already quite strong, the radiosonde profiles at that time were not used directly to initialize the simulations. The following steps show how we modify the 1D model profiles to avoid instabilities from lack of appropriate data.

a) Below height of 1500 m: to use U-wind and V-wind value of 1500 m;
b) If there are missing data of U-wind and V-wind in the high levels, to use the last recorded value of U-wind and V-wind;
c) Limit the vertical temperature gradient to −0.0095 K/m;
d) Above 6000 m height: set to stable stratification with a decrease rate of −0.0050 K/m of real air temperature;
e) Above 12000 m height: to use the relative humidity at 12000 m;

Limit the maximum relative humidity: 95% (0–2000 m), 80% (2000–5000 m), and 80% (above 5000 m). Fig. S1, Fig. S2, and Fig. S3 show the final humidity and wind profiles of each case.

2.2.4. *Surface cover data and land use change scenarios*

The original land use data used in this paper is based on the GlobCover (global land cover product delivered for the period between December 2004 and June 2006). The data has a 300 m resolution and 22 independent validation global (or level 1) legend land use categories

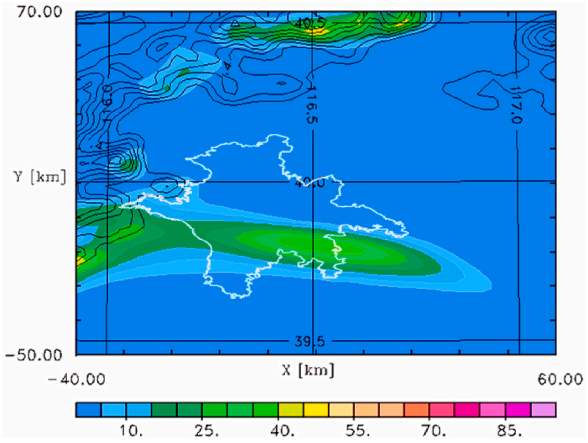

Fig. 6. Horizontal distribution of daily precipitation sum of the chosen Case One with the reference land use. The white line circled area roughly stands for the urban area based on the land-use data in 2010. (Unit: mm).

(Bicheron et al., 2008). We map the "urban" surface cover class in the GlobCover data onto the METRAS surface cover classes as following: 2% water, 7% grass, 4% bushes, 17% trees, 5% cropland, 5% asphalt, 35% low buildings(<= 12 m), and 25% high buildings (>12 m): based on the table of vegetation resources for Beijing (Green Resources, 2012), the governmental urban planning report (2004–2020) of Beijing (Urban planning report, 2007), and the map of building height of Beijing made by Tsinghua University. The reference scenario with the modified land use data used in the control experiment is shown in Table 2.

Main land use classes of the chosen domain are presented in different colors in Fig. 4. In total, we applied 18 land use categories in the simulations, including two types of urban defined as only consisting of buildings and adjacent sealed surfaces. Different land uses change the moisture, momentum, and heat exchange processes between the surface and atmosphere. In this study, we calculate the surface energy budget and all surface dependent fluxes with respect to the surface characteristics rather than employ a canopy sub-model. Table S2 in appendix lists the 18 classes' physical parameters.

The objective of this study is to explore the impacts of urbanization in Beijing on the summer precipitation and the potential mechanisms. To meet this objective, we investigated four sensitivity experiments with idealized scenarios of different urban land-use (Table 2) apart from the reference scenario introduced above.

The No-urban scenario and the Reference scenario are regarded as the pre-urban period state and the current urban state respectively. SCE_High, SCE_Expand, and SCE_Novegare help show whether the height of buildings or the urban expansion influence the local climate. In short, SCE_Refer and SCE_High have a similar city size but different building heights; while SCE_Expand has a larger size city with a less dense urban area and SCE_Noveg has a larger size city with a much denser urban area.

We simulated every selected heavy precipitation event five times with the five different scenarios for a total of 65 simulations.

3. Results and analysis

The spatial patterns of the mean differences of the sum precipitation over all cases between urban-scenarios (SCE_Refer, SCE_High, SCE_Expand, SCE_Noveg) and the rural-scenario (SCE_Nourb) are displayed in Fig. 5. The differences within each panel are random, and note the scale, these differences are all smaller than 1 mm which means nearly nothing. In general, it needs at least 40 years daily precipitation data to get a related precision climatological precipitation distribution, which is longer than temperature. Hence, it is not appropriate to analysis the precipitation changes by using the whole mean method as above. Schoetter (2013) did 72 meteorological situations of Hamburg with urban and no-urban scenarios. He found for a single meteorological situation there are large differences between two scenarios, but these differences cancel out when analyzing the ensemble of all 72 situations. And here Fig. 5 illustrates the same kind of result. The precipitation of each event should be analyzed independently.

As the whole climate system is interactional, changes in other components will influence precipitation indirectly. Precipitation responds directly or indirectly to changes of other meteorological parameters, it is a quite complex process including kinds of mechanisms. So for the rainfall differences in or near the urban area, it is hard to tell if they are related to the effects of the urban environment. The wind speed and direction are always changing, the influenced range by urban argues. Besides, the purely convection is sensitive to the local perturbation. After analyzing all 13 rain events results, the chosen two rain cases in this chapter are among those most likely to be influenced by the urban effects.

3.1. Case one

Case one is the precipitation process in the first day of the No.7 rain event of Table 1, the simulations are initialized at 20:00 CST on 1 August 2007 with the near surface air temperature of 30 °C and soil & water temperature of 26 °C. No precipitation has been recorded at the routine observation station at the days before the heavy precipitation event, therefore we choose the number of "dry days" as zero. The wind comes from west with a speed of about 4 m/s at the steering level of the clouds (around 700 hPa geopotential height).

The precipitation process happens during the night and it lasts to 7:00 in the morning. The clouds accompanied with rainfall are from the mountains, moving past the southern part of the urban area. The rainfall center is in the southeast of the urban area (Fig. 6). Although there is rainfall over the mountains, the effects of urbanization on precipitation are expected in the urban area or east of the urban area. In order to investigate the precipitation amount variations with time, the precipitation amounts between 39.6 and 40.0 °N of each longitude are integrated and shown in Fig. 7. The urban area of reference scenario is between about 116.1 and 116.5 °E, the SCE_Expand and SCE_Noveg have larger urban area.

Comparing Fig. 7(a) (SCE_Refer), Fig. 7(b) (SCE_Nourb) and Fig. 7(c) (SCE_High), it illustrates that although the general characteristics of the precipitation processes are similar, the intensity is different. SCE_Nourb has the most precipitation in the urban area and the least precipitation in the downwind area between about 116.7 and 116.8 °E. Besides, the rainfall of SCE_High is less than that of SCE_Refer. It seems the presence of the city has an influence on reducing the rainfall in the urban area especially the rougher city, and increasing the rainfall in the downwind area.

Contrasting the results across all the different urban land uses, it reveals that the rain clouds of both SCE_Expand and SCE_Noveg move more quickly than for the other land use scenarios, and the location of the maximum precipitation is about 50 km farther to the east. The two larger urban scenarios both have higher precipitation intensity. It seems that the urban area may affect the moving speed of rain clouds, and urban expansion may enhance the intensity of precipitation.

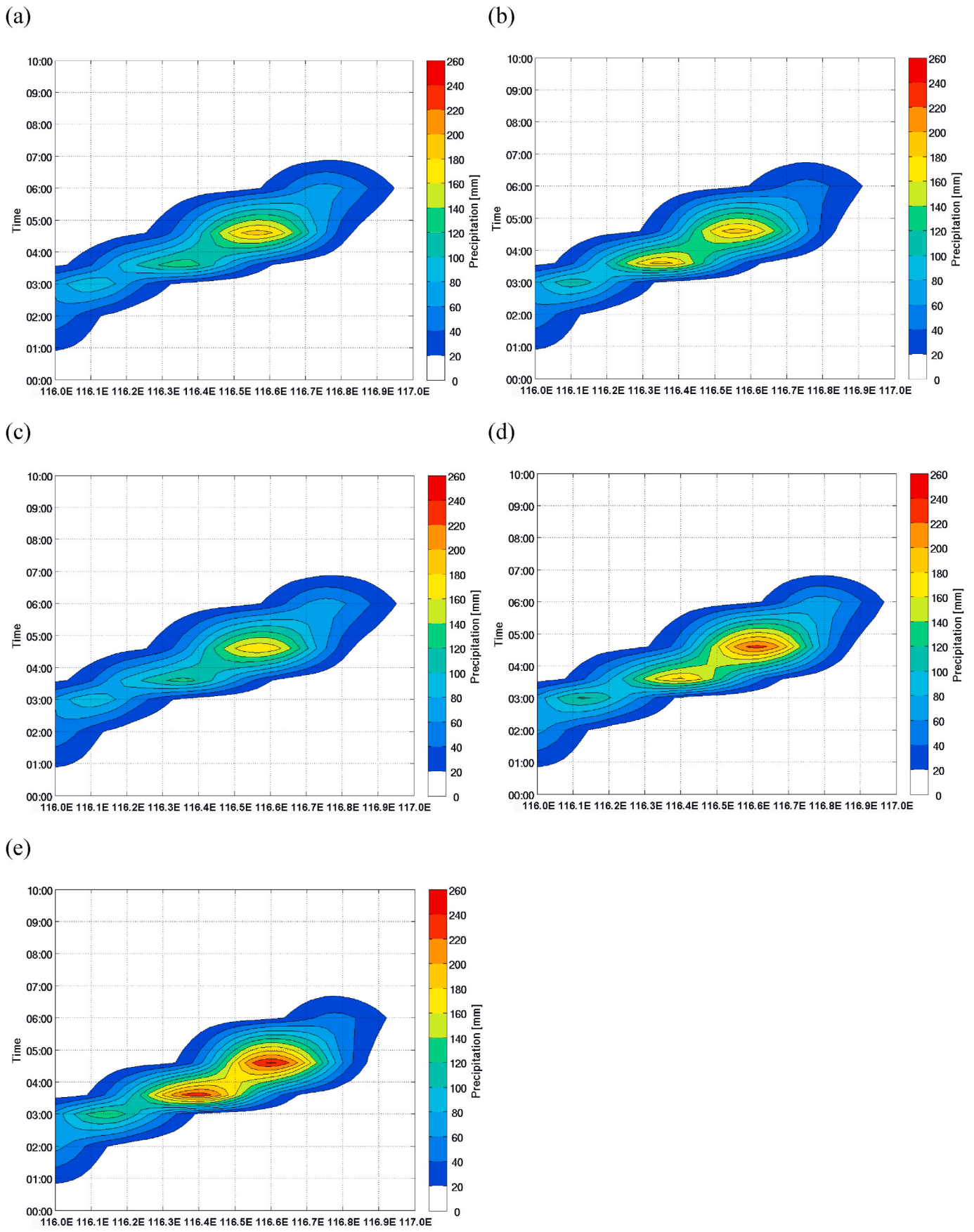

Fig. 7. Time evolution of the regional integrated precipitation of Event 7 in Table 1 a) SCE_Refer; b) SCE_Nourb; c) SCE_High; d) SCE_Expand; e) SCE_Noveg. (Unit: mm).

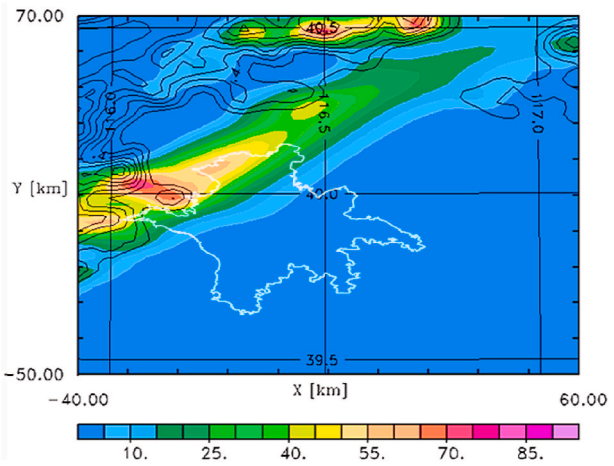

Fig. 8. Horizontal distribution of the daily precipitation sum of Case Two with the reference land use. The white line circled area roughly stands for the urban area based on the land-use data in 2010. (Unit: mm).

3.2. Case two

Case two is also the precipitation process in the first day but in the No.12 rain event of Table 1. The initialization time is 20:00 CST on 4 August 2011. The near surface air temperature is 26.4 °C which is much lower than that of Case one, and the soil & water temperature is 26 °C. There are four "dry days" before the simulated day, making the soil is relatively dry. The wind is the southwest with a speed of about 8 m/s, which is larger than that of Case one.

Fig. 8 shows the horizontal distribution of daily precipitation accumulation, which is located between 39.7 and 40.4°N. There are actually two rain events, one starts about 1:30 and ends at 4:30 distributed between 116.1 and 117.0 °E; the other starts over the mountains and passes through the northern part of the urban area.

Comparing all the subfigures in Fig. 9, for the first precipitation event, it can be seen that the rain of all urban scenarios in the urban area (116.1–116.3 °E) begins approximately 20 min earlier and lasts longer than that of the no-urban scenario. Note that the urban area of the reference scenario in Fig. 9 is between about 116.1 and 116.3 °E as the northern part of the urban area is narrow. In addition, all the urban scenarios give more precipitation in the downwind area than SCE_Nourb although the rain amount of SCE_Noveg is just a little larger than that of SCE_Nourb.

For the second precipitation process, the rain in the urban area of SCE_Nourb is the heaviest followed by that of SCE_Refer. The decline in rain volume is most obvious in Fig. 9(e). Moreover, there are some differences in the period 6:00–8:00 among the five scenarios. In the area of 116.3–116.6 °E, SCE_Refer, SCE_High and SCE_Expand have more rainfall than SCE_Nourb, however, SCE_Noveg has less rainfall.

4. Discussion and conclusions

In summary, the urbanization of Beijing has certain influences on the precipitation process, but the magnitude of the influence depends on various factors. It is inappropriate to claim that the changes of rainfall over time is correlated to urbanization. Many factors affect the precipitation, such as large-scale atmospheric variability. The precipitation of each event should be analyzed independently. Case one and Case two both show the rain amount in the urban area decreases, which is possibly because of the increased water-holding capacity of the atmosphere and the decreased evaporation in the urban areas. We do find more rain falls in the downwind region. This may be because there is more water vapor in the atmosphere in the urban area, and as warmer air can hold more water before becoming saturated, the evaporated water must fall as rain in the downwind area.

The increase of urban size or density may speed up the movement of rain clouds. Urbanization leads to increased surface roughness, which enhances the low-level convergence and upward vertical velocities (Diem and Mote, 2005). The enhancing of UHI-circulation is not only embodied in the upward, vertical velocities but also the horizontal ones. Moreover, stronger precipitation intensity in the urban area also exists, which means in some cases urban expansion could give rise to heavier precipitation or extreme rain events. It is also worth noting that we find the rainfall of SCE_High is less than that of SCE_Refer in both cases. This may be because of the urban barrier effect. The higher urban area may disrupt or bifurcate the clouds as a whole, suppressing the development of the convective system. Due to the lack of extensive previous studies, further in-depth modeling studies would help understand the mechanisms involved in the impact of higher buildings on precipitating convective system. Since the anthropogenic heat and aerosols have not been taken into account in this study, the increase of anthropogenic aerosols may result in the increase of concentration of cloud condensation nuclei, which would correspond to clouds that become larger and last longer. The impact of anthropogenic aerosols on clouds and the cloud feedback is still a big uncertainty as illustrated in the Fourth Assessment Report of the Intergovernmental Panel on Climate Change (IPCC). The real precipitation process will be more complex and the changes should be greater.

The findings and conclusions are summarized as following:

1) There is nearly no difference of the precipitation sum of all 13 simulated rain events between urban-scenarios (SCE_Refer, SCE_High, SCE_Expand, SCE_Noveg) and the rural-scenario (SCE_Nourb). The effects of urbanization on the precipitation can only be found in single cases.
2) For the precipitation events passing through the city, the presence of the urban area has an effect on reducing the rainfall in the urban area and increasing rainfall downwind of the urban area. However, heavier rain events exist in some cases, which means extreme precipitation events could be more common in response to the urban expansion.
3) The urban pattern significantly impacts the rainfall area and intensity. The increased urban size or density may speed up the movement of rain clouds while the increased urban height may disrupt or bifurcate the clouds.

In the future, the changes of extreme precipitation frequency and precipitation distribution should be investigated based on the observational data. Besides, the land use scenarios are idealized, it will be much better to implement more accurate land-use data in the nested modeling simulations. Since anthropogenic heat and pollution release are important factors to urban precipitation, they should be included in the modeling too, leading to more realistic simulation results. Finally, more rain events of different types (e.g., cyclonic rainfall, typhoon rainfall) should be simulated and analyzed in order to increase the confidence of conclusions on urban precipitation as well as the understanding of precipitation mechanisms.

CRediT authorship contribution statement

Jingru Liu: Conceptualization, Methodology, Data curation, Writing – original draft, Visualization, Investigation. **K. Heinke Schlünzen:** Conceptualization, Methodology, Supervision, Writing – review & editing. **Thomas Frisius:** Supervision, Writing – review & editing. **Zhan Tian:** Writing – review & editing.

Declaration of competing interest

The authors declare that they have no known competing financial interests or personal relationships that could have appeared to influence the work reported in this paper.

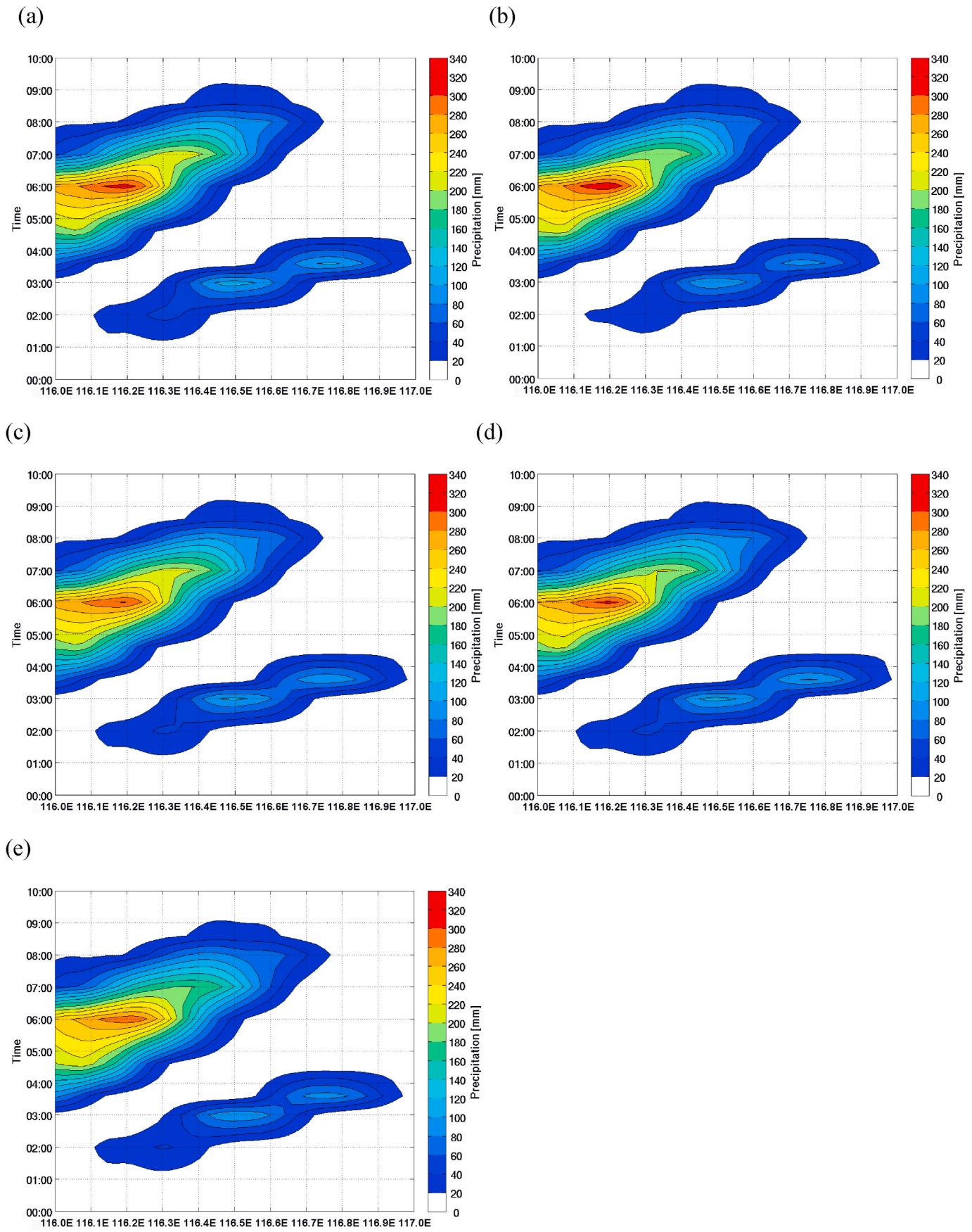

Fig. 9. Time evolution of the regional integrated precipitation of Event 12 in Table 1 a) SCE_Refer; b) SCE_Nourb; c) SCE_High; d) SCE_Expand; e) SCE_Noveg. (Unit: mm).

Acknowledgements

This work was supported by the National Key R& D Program of China (2019YFE0124800), High-level Special Funding of the Southern University of Science and Technology (Grant no. G02296302, G02296402). We also would like to show our gratitude to University of Hamburg, German Meteorological Service (DWD), Max-Planck-Institute of Meteorology (MPI-M) and Southern University of Science and Technology. We thank Austin Sandler for his efforts in improving our exposition.

Appendix A. Supplementary data

Supplementary data to this article can be found online at https://doi.org/10.1016/j.pce.2021.103005.

References

Bicheron, P., Defourny, P., Brockmann, C., Schouten, L., Vancutsem, C., Huc, M., Bontemps, S., Leroy, M., Achard, F., Herold, M., Ranera, F., Arino, O., 2008. GLOBCOVER: Products Description and Validation Report. Medias France.

China City Statistical Yearbook, 2017. Retrieved september 12, 2020 from the website:. https://wenku.baidu.com/view/d7c05beef56527d3240c844769eae009581ba299.html.

Diem, J.E., Mote, T.L., 2005. Interepochal changes in summer precipitation in the southeastern United States: evidence of possible urban effects near Atlanta, Georgia. J. Appl. Meteorol. 44 (5), 717–730.

Guo, X., Fu, D., Wang, J., 2006. Mesoscale convective precipitation system modified by urbanization in Beijing City. Atmos. Res. 82 (1), 112–126.

Grawe, D., Thompson, H.L., Salmond, J.A., Cai, X.M., Schlünzen, K.H., 2013. Modelling the impact of urbanisation on regional climate in the Greater London Area. Int. J. Climatol. 33, 2388–2401. https://doi.org/10.1002/joc.3589.

Green resources table of Beijing in 2011, 2012. Retrieved november 25, 2013 from the beijing municipal Bureau of landscape and forestry website:. http://www.bjyl.gov.cn/zwgk/tjxx/201203/t20120330_104521.html.

Hand, L.M., Shepherd, J.M., 2009. An investigation of warm-season spatial rainfall variability in Oklahoma City: possible linkages to urbanization and prevailing wind. J. Appl. Meteorol. Climatol. 48 (2), 251–269.

Lin, B.Q., 2000. Urban heat islands and summertime convective thunderstorms in atlanta: three case studies. Atmos. Environ.

Lei, M., Niyogi, D., Kishtawal, C., Pielke, R.A., Beltrán-Przekurat, A., Nobis, T.E., et al., 2008. Effect of explicit urban land surface representation on the simulation of the 26 july 2005 heavy rain event over Mumbai, India. Atmos. Chem. Phys. Discuss. 8 (20), 5975–5995.

Mote, T.L., Lacke, M.C., Shepherd, J.M., 2007. Radar signatures of the urban effect on precipitation distribution: a case study for Atlanta, Georgia. Geophys. Res. Lett. 34 (20), L20710.

Mu, F., Zhang, Z., Liu, B., Wang, C., 2007. Remote sensed monitoring of land use change in Beijing based on TM images and "Beijing-1". Ecol. Environ. 1.

Niyogi, Dev, Patrick, Pyle, Lei, Ming, et al., 2011. Urban modification of thunderstorms: an observational storm climatology and model case study for the indianapolis urban region. J. Appl. Meteorol. Climatol.

Rozoff, C.M., Cotton, W.R., Adegoke, J.O., 2003. Simulation of St. Louis, Missouri, land use impacts on thunderstorms. J. Appl. Meteorol. 42 (6), 716–738.

Schneider, A., Metres, C.M., 2014. Expansion and growth in Chinese cities 1978-2010. Environ. Res. Lett. 9, 024008, 11.

Schlünzen, K.H., 1990. Numerical studies on the inland penetration of sea breeze fronts at a coastline with tidally flooded mudflats. Contrib. Atmos. Phys. 63 (3–4), 243–256.

Schlünzen, K.H., Hoffmann, P., Rosenhagen, G., Riecke, W., 2010. Long-term changes and regional differences in temperature and precipitation in the metropolitan area of Hamburg. Int. J. Climatol. 30 (8), 1121–1136.

Schlünzen, K.H., Flagg, D.D., Fock, B.H., Gierisch, A., Lüpkes, C., Reinhardt, V., Spensberger, C., 2012. Scientific documentation of the multiscale model system M-SYS (METRAS, MITRAS, MECTM, MICTM, MESIM). Meteorologisches Institut, KlimaCampus, Universität Hamburg. – MEMI Technical Report 4.

Schoetter, R., 2013. Can Local Adaption Measures Compensate for Regional Climate Change in Hamburg Metropolitan Region? Doctoral dissertation, Universität Hamburg).

Shepherd, J.M., Burian, S.J., 2003. Detection of urban-induced rainfall anomalies in a major coastal city. Earth Interact. 7 (4), 1–17.

Sun, J., 2007. The effect of urban heat island on winter and summer precipitation in Beijing region. Chin. J. Atmos. Sci. 2.

Taylor, C.M., de Jeu, R.A., Guichard, F., Harris, P.P., Dorigo, W.A., 2012. Afternoon rain more likely over drier soils. Nature 489 (7416), 423–426.

Xing, Y., Liu, J.H., Ni, G.H., 2020. Impacts of urban canopy roughness on storm evolution and rainfall area. J. Tsinghua Univ. (Sci. Technol.) 60 (10), 845–854.

Yue, C.J., Tang, Y.Q., Gu, W., et al., 2019. Study of urban barrier effect on local typhoon precipitation. Meteorol. Mon. 45 (11), 1611–1620. https://doi.org/10.7519/j.issn.1000-0526.2019.11.011.

Yang, P., Ren, G.Y., Yan, P.C., 2017. Evidence for strong association of short-duration intense rainfall with urbanization in Beijing urban area. J. Clim. 30 (15).

Yang, S.H., Ma, L., Chen, S., 2009. Interaction of spatial structure evolution and urban transportation. Urban Trans. China 5, 010.

Yuan, Y.F., Zhai, P., Chen, Y., Li, J., 2020. Hourly Extreme Precipitation Changes under the Influences of Regional and Urbanization Effects in Beijing. Royal Meteorology Society.

Zhang, J., Zhou, Y.S., Shen, X.Y., 2020. Numerical simulation analysis of the impact of urbanization on an extreme precipitation event over beijing–tianjin–hebei, China. Atmosphere 11 (9), 945, 2020.

Zhao, P., 2010. Sustainable urban expansion and transportation in a growing megacity: consequences of urban sprawl for mobility on the urban fringe of Beijing. Habitat Int. 34 (2), 236–243.

Zheng, S.Y., Liu, S.H., 2008. Urbanization effect on climate in beijing. Clim. Environ. Res. 2.

Zhang, Y., Smith, J.A., Luo, L.F., Wang, Z.F., Baeck, M.L., 2014. Urbanization and rainfall variability in the beijing metropolitan region. J. Hydrometeorol. 15 (6), 2219.